



Succession of microbiota and its influence on the dynamics of volatile compounds in the semi-artificial inoculation fermentation of mulberry wine

Yanan Qin^{a,1}, Haotian Xu^{a,1}, Jinshuai Sun^a, XiangYang Cheng^a, Jing Lei^b, Weijia Lian^b, Chen Han^b, Wanting Huang^a, Minwei Zhang^a, Ya Chen^{b,*}

^a Xinjiang Key Laboratory of Biological Resources and Genetic Engineering, College of Life Science & Technology, Xinjiang University, Urumqi 830046, China

^b Turpan Institute of Agricultural Sciences, Xinjiang Academy of Agricultural Sciences, Turpan 838000, China

ARTICLE INFO

Keywords:

Mulberry wine
Semi-artificial inoculation fermentation
Microbiota community
Volatile compounds
Correlation analysis

ABSTRACT

To improve the delightful flavor of mulberry wine through semi-artificial inoculation fermentation with *Saccharomyces cerevisiae*, we studied the dynamics change of microbiota, along with the physicochemical properties and metabolite profiles and their interaction relationship during the fermentation process. The abundance of lactic acid bacteria (*Weissella*, *Lactobacillus*, *Fructobacillus*, and *Pediococcus*) increased significantly during fermentation, while yeasts gradually established dominance. The inter-kingdom network of the dominant genera analysis further identified the following as core microbiota: *Alternaria*, *Botrytis*, *Kazachstania*, *Acremonium*, *Mycosphaerella*, *Pediococcus*, *Gardnerella*, and *Schizothecium*. Additionally, pH, alcohol, and total acid were significantly affected by microbiota variation. Fourteen of all identified volatile compounds with key different aromas were screened using PCA, OPLS-DA, and rOAV. The network of interconnected core microbiota with key different aromas revealed that *Kazachstania* and *Pediococcus* had stronger correlations with 1-butanol, 3-methyl-, propanoic acid, and 2-methyl-ethyl ester.

1. Introduction

Mulberries (*Morus nigra*. L) have a long-standing cultivation history in the northwestern region of China, particularly in Xinjiang, where a temperate continental climate prevails (Ercisli & Orhan, 2007). Geographical characteristics such as aridity, ample sunlight, and substantial diurnal temperature variations create favorable conditions for the transportation, transformation, and accumulation of secondary metabolites within the plant kingdom (Hosseini et al., 2018). In response to the local environment, mulberries cultivated in southern Xinjiang have acquired notable traits such as drought tolerance, prolonged fruit maturation, and distinctive physicochemical attributes (Jiang & Nie, 2015). Although consumed fresh, the perishable nature of local mulberries necessitates their processing into mulberry wine. For instance, mulberry wine aligns with the policy shift of the Chinese alcoholic beverage industry towards reduced grain consumption and low alcohol content. Compared with raw mulberries, mulberry wine offers a richer taste and aroma. Moreover, mulberry wine significantly increases total phenolic content and antioxidant activity (Zhang et al.,

2022). Therefore, the amalgamation of the aforementioned advantages of mulberry fermentation into fruit wine not only enriches fruit wine varieties but also provides consumers with various choices, possessing a vast development space and market potential.

Semi-artificial inoculated fermentation, facilitated by incorporating specific starter cultures such as *Saccharomyces cerevisiae*, offers significant advantages in terms of precise regulation of the fermentation process and enhanced refinement of the resulting fermented products (Su et al., 2020; Teng et al., 2021). Furthermore, this modality of fermentation greatly stimulates the metabolic activity associated with the thriving microbial consortia in the fermentation milieu, thereby accumulating various aromatic compounds in the end products of fermentation. Aroma—a fundamental manifestation of food quality attributes—is crucial in determining the market positioning and consumer acceptance of a food product (Ristic et al., 2019). Studies have shown that both *non-Saccharomyces cerevisiae* and *Saccharomyces cerevisiae* are crucial in the formation of volatile flavor profiles, particularly sophisticated alcohols and esters, in “NanFeng tangerine wine” and “Merlot wine” (Liang et al., 2023; Yang et al., 2022). Furthermore, lactic

* Corresponding author.

E-mail address: chenya1107@sina.com (Y. Chen).

¹ Those authors equally contributed to this paper.

acid bacteria, along with *Saccharomyces cerevisiae* strains introduced through conventional brewing methods, and filamentous fungi substantially influence the sensory characteristics of “Sesotho” and “Cabernet Sauvignon (*Vitis vinifera* L.) wines (Cason et al., 2020; Wei et al., 2022). The bacterial strains significantly affect the formation and conversion of unique volatile compounds. Furthermore, the predominance of lactic acid bacteria as the dominant microbial population controls harmful pathogens and inhibits spoilage microorganisms, thereby preserving wine quality (Cason et al., 2020). However, few studies have probed such relationships during mulberry wine fermentation. Current research on mulberry wine has focused on exploring its clarifying effectiveness, processing methods, and functional properties (Ekumah et al., 2021; Hu et al., 2021; Zhang et al., 2022). Nevertheless, few studies have examined the complex interaction between microbial community dynamics and their subsequent effect on the sensory characteristics of mulberry wine. Consequently, the succession of microbial communities during the semi-artificial fermentation process of mulberry wine substantially influences the formation of crucial aroma compounds.

Therefore, the present study explored the relationship between microbiota communities and volatile compounds during mulberry wine fermentation. The succession of microbiota communities and the change in volatile compounds were analyzed through high-throughput sequencing (HTS) and headspace-solid phase microextraction gas chromatography-mass spectrometry (HS-SPME-GC-MS) techniques, respectively. Meanwhile, the core microbiota and their effects on environmental factors were detected by a network of inter-kingdom and redundancy analysis (RDA), respectively. The results may contribute to a clearer understanding of the role of local microorganisms in forming key aromas and developing starters to improve the regional characteristics of fruit wines.

2. Material and methods

2.1. Materials

All chemicals were of analytical grade. 2-Octanol was obtained from TCI (Shanghai, China). HCl (1 + 1 (v/v)), NaOH (200 g/L), glucose standard solution (2.5 g/L), methylene blue (10 g/L), phenolphthalein, CuSO₄ (0.05 g/mL), and NaOH (0.05 mol/L) were obtained from Macklin (Shanghai, China). The dry yeast (*Saccharomyces cerevisiae* DV 10) was obtained from JATOU (Shanghai, China).

2.2. Semi-artificial inoculated fermentation and sample collection

In May 2022, black mulberry fruits were harvested from the Turpan area, Xinjiang Province, China. The mature, high-quality mulberries, without rot or mildew, were used in the subsequent fermentation process.

The semi-artificial inoculation fermentation was conducted in the small-scale production line at an ambient temperature of 20 °C. Fruit juice (pulp) was extracted from mulberry fruits using a belt press; the pulp was then transferred to a fermenter, where SO₂ (0.03 g/L) and pectinase (0.02 g/L) were added. Subsequently, 0.25 g/L of activated *Saccharomyces cerevisiae* DV10 (LALVIN, Denmark) was added to the musts at the bottom of the fermentation tank. At the onset of fermentation, FERMAID E (0.15 g/L) was introduced as a fermentation nutrient, which was added again after 7 d (at 0.15 g/L). After 12 d, the fermentation process was terminated by adding SO₂ (0.06 g/L). The alcohol content should be 10 v/v % (semi-sweet type) by the end of fermentation.

Samples were collected during the fermentation process at 0, 24, 36, 72, 168, and 288 h (for each time point, samples were obtained from the fermenter's top, middle, and bottom surfaces). The mixed samples were then divided into three parts and stored at -80 °C for oenological parameters, microbial community structure, and HS-SPME-GC-MS

analysis.

2.3. Oenological parameters

The following physicochemical parameters of the samples were determined: pH, Brix, total acid, total sugar, and alcohol content. The pH was measured using a digital benchtop pH meter (PHS-3C, Shanghai, China). The total acid (TA) content was determined through potentiometric titration, with a pH of 8.2 serving as the endpoint for the titration. The total soluble solid (TSS) content was measured using a hand-held Brix meter. The alcohol content was determined using the alcohol meter method (M277465, China). Total sugar (TS) content was determined by direct titration. The calculation formula is as follows: $TS = F \times 1000 / ((V_1/V_2) \times V_3)$. Where, TS is total sugar content (g/L), F (g) is the number of grams of glucose corresponding to 5 mL of each of Fehling's solution (I, II), V₁ (mL) is the volume of the sample taken, V₂ (mL) is the volume of sample diluted, V₃ (mL) is the volume of the consumed sample. The specific instruments and procedures are described in our previous paper (Qin et al., 2023).

2.4. DNA extraction, qualification, and microbial community analysis

DNA was extracted from fermentation broth (0.5 mL) using the DNeasy PowerSoil Kit (QIAGEN, Inc., Netherlands), following the manufacturer's instructions, and subsequently stored at -80 °C for subsequent analysis. The concentration and purity of the extracted DNA were assessed using the NanoDrop ND-1000 spectrophotometer (Thermo Fisher Scientific, Waltham, MA, USA), whereas agarose gel electrophoresis was used to evaluate the DNA's quality. We amplified the ITS1 regions (ITS5-1737F (GGAAGTAAAAGTCGTAACAAGG) and ITS2-2043R (GCTGCGTTCTTCATCGATGC)) and the 16S rRNA genes (V3-V4 regions 515F (CCTAYGGGRBGCASCAG) and 806R (GGACTACNNGGTATCTAAT)). Raw Tags were obtained by splicing the sample reads using the FLASH software. The Arch software was used to obtain the final adequate data. The 16S region uses SILVA138.1 database annotations, and the ITS region uses UNITEV8.2 database annotations. For the aforementioned effective tags, the DADA2 module in the QIIME2 software was used for noise reduction, and sequences with abundance < 5 were filtered out to obtain the final ASVs (amplicon sequence variants) and a feature list. The resulting ASVs were compared with the database using the classify-sklearn module in QIIME2 to obtain species information for each ASV.

2.5. Analysis of volatile compounds

The volatile compounds in the samples were analyzed using HS-SPME-GC-MS. In the SPME cycle of the PAL rail system. Fiber type: polydimethylsiloxane fiber; Incubate temperature: 60 °C; Preheat time: 15 min; Incubate time: 30 min; Desorption time: 4 min. The analysis was conducted using a gas chromatograph system (Agilent 7890, California, USA) coupled with a mass spectrometer (Agilent 5977B, California, USA). As an internal standard, 10 µL of 2-Octanol (TCI, Shanghai, China) (10 mg/L stock in dH₂O) was added into a 20 mL headspace bottle containing 100 µL of thawed sample. The GC procedure was as follows: Helium was used as the carrier gas, with a front inlet purge flow rate of 3 mL/min and a gas flow rate of 1 mL/min through the column. The initial temperature was maintained at 40 °C for 4 min, followed by a programmed increase to 245 °C at a rate of 5 °C/min, and finally held for 5 min. The injection, transfer line, ion source, and quad temperatures were set at 250, 250, 230, and 150 °C, respectively. Electron impact mode was used with an energy of -70 eV. Mass spectrometry data were acquired in scan mode spanning the m/z range of 20-400 with a solvent delay of 0 min (Additional mass spectrometry parameters in Chroma TOF software: Peak width: 3, S/N ratio: 10, baseline offset: 0.5). NIST 17.0 Mass Spectral Library (<https://chemdata.nist.gov>) and Chroma TOF 4.3X software (Michigan-based LECO Corporation, USA), with

assistance of references (Garcia & Barbas, 2011), were employed for raw peak extraction, baseline filtering, baseline correction, peak alignment, deconvolution analysis, peak identification, integration, and spectral matching. These procedures facilitated the qualitative and quantification identification of volatile compounds.

2.6. Calculation of rOAV

The key volatile compounds are expressed as relative odor activity values (rOAV), which are calculated from the relative concentrations of volatile compounds at 0 and 288 h during fermentation using the following equation:

$$rOAV_i = 100 \times \frac{C\%_i}{C\%_{\max}} \times \frac{T_{\max}}{T_i}$$

where $C\%_{\max}$ is the compound with the maximum relative percentage content, and T_{\max} is the threshold value for $C\%_{\max}$. $C\%_i$ is the relative content (%) of the target volatile compounds, and T_i is the odor threshold for $C\%_i$ in water. $rOAV > 1$ is considered the key aromatic compound. The greater the rOAV value, the greater the component's contribution to the sample's overall flavor profile. Fractions with $rOAV \geq 1$ were considered the key flavor compounds of the analyzed samples, and fractions with $0.1 \leq rOAV < 1$ had a vital modifying effect on the sample's overall flavor profile (Zhang et al., 2019).

2.7. Statistical analysis

Statistical analyses were performed using the SPSS 21.0 software (IBM SPSS Inc., Chicago, Michigan, USA). The alpha diversity of the microbial communities was assessed using the Chao 1 and Shannon indices, which were computed using the appropriate functions within the R package. Principal coordinate analysis (PCoA) was used to evaluate the distribution patterns of the microbial communities. ANOSIM and permutation multivariate analysis of variance (PMANOVA) were performed to determine the significant differences between the sample groups based on Bray–Curtis distance matrices. The definition of the core microbiota was illustrated using “igraph”. OPLS-DA was used with the SIMCA 14.1 package (Sartorius Stedim Data Analytics AB, Umea, Sweden). Microbial and volatile components histograms were created using Origin 2021pro software (OriginLab Corp., Northampton, MA, USA) and Microsoft Excel 2019 (Microsoft Windows Office, USA). Additionally, RDA was used to analyze the correlation between oenological parameter variables and the core microbiota in the “vegan” R package. Network visualization was used to clarify the correlation between the core microbiota and the key differential aromas in mulberry wine fermentation, performed using Gephi (v0.9.5).

3. Results and discussion

3.1. Oenological parameter analysis

Table 1 presents the pH, TA, TS, TSS, and alcohol content of mulberry wine during its fermentation process. The pH (4.76), TA (3.99 g/L

tartaric acid), TS (69.36 g/L), and TSS (16.80 %) were recorded at the onset of fermentation (0 h). As the microbial community proliferates extensively, carbohydrates, proteins, and lipids undergo enzymatic transformations mediated by microbial enzymes (Carpena et al., 2021). These enzymatic processes, coupled with adsorption and flocculation phenomena occurring in the fermentation substrate, convert macromolecular organic substances into small-molecule organic compounds (e.g., lactic acid, tartaric acid, malic acid, succinic acid, citric acid, and acetic acid) and polymeric metabolites (Yuan et al., 2022). Consequently, these metabolic products influence the surrounding oenological parameters. At 288 h, the pH and TS decreased to 3.91 and 57.51 g/L, respectively. Contemporarily, TA increased to 13.76 g/L, and TSS reached 20.57 %. Notably, the absence of alcohol content was observed within 72 h and subsequently increased gradually to 10 v/v %. *Saccharomyces cerevisiae* DV10 and non-*Saccharomyces cerevisiae* (the facultative anaerobic), with strong adaptability to anaerobic oenological parameters (Escribano-Viana et al., 2018), extensively grow and metabolize after 72 h and begin to produce alcohols.

3.2. The microbial succession during mulberry wine fermentation

The 16S rRNA gene's V3-V4 region was sequenced in 18 samples, resulting in 1,137,862 high-quality reads (QIIME, 2.0) available for subsequent analysis. On average, each sample contained 63,214 sequences. After excluding low-abundance and non-bacterial ASVs, clustering with a similarity threshold of 97.00 % produced 2,693 ASVs. In the case of fungi, high-throughput sequencing generated 1,357,048 high-quality reads, with an average of 75,391 sequences per sample, leading to the identification of 581 ASVs (similarity threshold of 97.00 %). The diversity and richness of microorganisms, as determined using the Shannon and Chao indices, are illustrated in Fig. S1. Notably, the bacterial richness and diversity were significantly higher during the 0–36 h period compared with the 72–288 h period, whereas the opposite trend was observed for fungi. Perhaps attributable to diverse microbial coexistence within the fermentation environment, lactic acid bacteria proliferate, and their metabolic activities generate a substantial amount of lactic acid and other acidic substances as the fermentation progresses (0–72 h). Consequently, the pH gradually decreases, imposing acid pressure on the fermentation system. Under such conditions, lactic acid bacteria and acid-tolerant fungi dominated the microbial community structure within the entire fermentation system.

The application of PMANOVA validated the presence of significant differences in the microbiota communities among at least two samples during the fermentation process (bacteria, $R^2 = 0.6581$, $P = 0.008$; fungi, $R^2 = 0.7503$, $P = 0.001$). The PCoA results based on Bray-Curtis distance revealed that the microbial communities involved at 0, 24, 36, 72, 168, and 288 h could be separated and differentiated. For fungi communities, the first two principal coordinate (PC) axes accounted for 93.99 % of the overall variation, whereas these axes explained 81.85 % of the total variation for bacterial communities (Fig. 1A–B).

The results at the genus level revealed that *Weissella* (50.20 %–75.30 %) was the main bacteria in the fermentation process, and other bacterial genera, including *Lactobacillus* and *Zymobacter*, were present with

Table 1
Changes in physicochemical indexes during mulberry wine fermentation.

| Physicochemical indexes | Fermentation procedures | | | | | |
|-------------------------|-----------------------------|-----------------------------|-----------------------------|-----------------------------|-----------------------------|-----------------------------|
| | 0 h | 24 h | 36 h | 72 h | 168 h | 288 h |
| pH | 4.763 ± 0.006 ^a | 4.137 ± 0.006 ^b | 4.053 ± 0.006 ^c | 3.933 ± 0.006 ^d | 3.923 ± 0.006 ^{cd} | 3.913 ± 0.006 ^e |
| TA (g/L) | 3.993 ± 0.185 ^e | 8.550 ± 0.375 ^d | 9.6267 ± 0.072 ^c | 12.357 ± 0.394 ^b | 12.460 ± 0.428 ^b | 13.757 ± 0.571 ^a |
| TS (g/L) | 69.356 ± 1.542 ^a | 69.881 ± 1.780 ^a | 55.436 ± 2.082 ^b | 68.875 ± 2.298 ^a | 55.873 ± 3.693 ^b | 57.505 ± 2.642 ^b |
| TSS (%) | 16.833 ± 0.153 ^a | 17.267 ± 0.115 ^a | 19.600 ± 0.100 ^b | 19.867 ± 0.116 ^b | 20.967 ± 0.153 ^c | 20.567 ± 0.404 ^d |
| Alcohol (v/v, %) | n.d. | n.d. | n.d. | 3.467 ± 0.153 ^c | 8.533 ± 0.058 ^b | 10 ^a |

Note: Data are presented as mean ± standard deviation (n = 3); a-e: Different lowercase letters indicated significant differences between the samples ($P < 0.05$, one-way ANOVA); Total acid expressed as tartaric acid; n.d.: not detected.

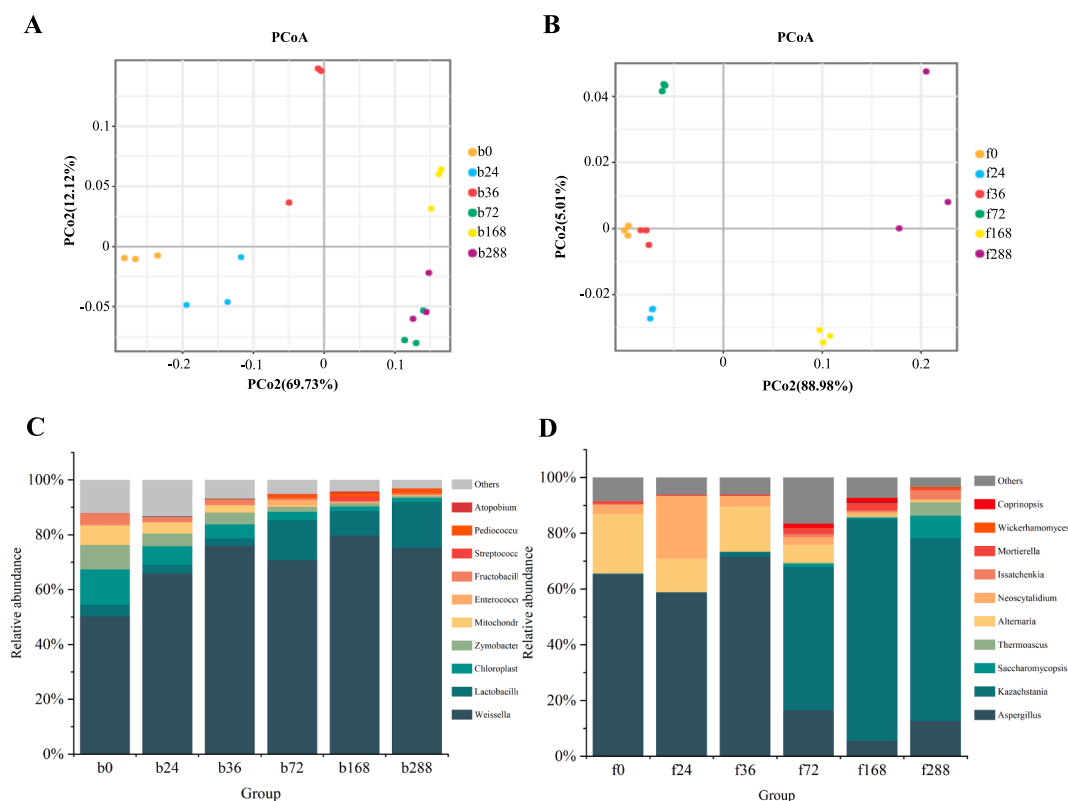


Fig. 1. The microbial community dynamics during mulberry wine fermentation. PCoA shows the bacterial community based on Bray-Curtis distance (A) and the fungi community based on Bray-Curtis distance (B) of samples during fermentation. The stacked column plots show the relative abundance changes of the dominant bacterial taxa (C) and fungi taxa (D) (Top 10 relative abundance shown; ANOVA, $P < 0.05$).

varying proportions. The main taxa (top 10) from different time points were tracked, which revealed the dynamics and succession of the fungal and bacterial communities during the fermentation procedures. The stacked column plots showed that with the fermentation process, the bacteria taxa displayed significantly different relative abundance (Fig. 1C, $P < 0.05$). In the 0-h samples, we found various bacteria taxa, such as *Weissella*, *Lactobacillus*, *Zymobacter*, *Enterococcus*, and *Pediococcus*—the taxa with the highest overall percentage—reached an abundance percentage of 58.56 %. After 72 h, lactic acid bacteria extensively use the carbon sources in the fermentation liquid, resulting in the significant activation and expression of glycolysis-related enzymes, such as glucokinase, dehydrogenase, and lactate dehydrogenase, initiating the malolactic fermentation and promoting the acid reduction process (Tian et al., 2021; Wang et al., 2021). Disrupting the microenvironment balance leads to the gradual collapse of other bacterial groups under acidic stress (Tian et al., 2021). Until the end of fermentation, their relative abundance reached increased to 94.28 %, which promoted the generation of desirable flavor compounds (Wang et al., 2022). Notably, the relative abundance of *Enterococcus*—a genus predominantly composed of opportunistic pathogens—decreased during the fermentation process (0.3 %–0.1 %). This shift may be attributed to the transition of the dominant genus, with lactic acid bacteria playing a primary role, occupying the ecological niche within the microenvironment. Such alterations in bacterial abundance or community composition highlight the advantages of semi-artificial inoculation fermentation over spontaneous fermentation. For instance, in naturally fermented wine, the abundance of potential pathogenic bacteria such as *Acinetobacter*, *Pseudomonas*, and *Sphingobacterium* remains relatively stable throughout the fermentation process (Cason et al., 2020). Notably, the diversity of bacterial communities gradually decreased in our semi-artificially inoculated fermentation process (Supplementary Fig. S1)

towards the end of fermentation. By contrast, the diversity of bacterial communities in naturally fermented fruit wine remains stable throughout the fermentation process, whereas the diversity of fungal communities, crucial for alcohol fermentation, gradually declines as fermentation progresses (Cason et al., 2020). The fungal communities include mainly fermented yeast (*Kazachstania*, *Issatchenkia*, *Saccharomyces*, and *Wickerhamomyces*), filamentous fungi (*Mortierella*, *Alternaria*, *Neoscytalidium*, *Thermoascus*, and *Aspergillus*), and basidiomycetes (*Coprinopsis*). In the early stages of fermentation (0–36 h), most fungi were not fermented yeast. For instance, *Aspergillus* and *Alternaria* from the surface of the raw material were the main taxa at 0–36 h, ranging from 65.10 % to 71.50 % and 21.40 % to 16.30 %, respectively (Fig. 1D, $P < 0.05$). These fungi were strongly correlated with butane-1-ol, 2-pentanone, and dimethyl sulfide (Wen et al., 2021). Over time, non-*Saccharomyces cerevisiae* become more susceptible to changes in fermentation rate, ethanol production, and heat generation caused by the growth of *Saccharomyces cerevisiae*, owing to their oxidative and weak fermentative metabolism. Moreover, their tolerance to anaerobic conditions was also lower, leading to their inability to sustain viability and eventual substitution by fermenting yeast (Liu et al., 2022). Consequently, the fungal community shifts towards a predominance of fermentative yeasts within the fungal group. In 72 h and later, the relative proportion of most fermented yeasts increased significantly. *Kazachstania*, *Saccharomyces*, and *Issatchenkia* were the dominant fungal taxa associated with fermentation. Especially, *Kazachstania* was significantly enriched from 51.30 % to 65.50 % (Fig. 1D). Our results demonstrated that the fermentation sample at 168 h significantly produced several aroma-producing fermented fungi, allowing them to produce a more characteristic aroma via the interplay of multiple beneficial fungi in the later stage of fermentation. Towards the end of fermentation, the relative abundance of yeast reached its peak, exceeding 70 %, consistent with the natural fermentation model.

However, in contrast to the significant reduction in fungal diversity observed in spontaneous fermentation (Cason et al., 2020), an increase in fungal diversity was shown in our semi-artificially fermented mulberry wine. This could be attributed to the synergistic growth or co-metabolic effects between *Saccharomyces cerevisiae* and other species, which would offer a better environment for the fungal community (Liu et al., 2022). Meanwhile, the higher fungal diversity may contribute to enhancing the aromatic profile of mulberry wine. Moreover, the unique genus, with a higher percentage of retained bacteria, interacting with these fungi can produce more pleasant odors (Liu et al., 2023). Moreover, the unique genus, with a higher percentage of retained bacteria, interacting with these fungi can produce more pleasant odors (Liu et al., 2023).

3.3. The core microbiota of mulberry wine fermentation

In the present study, a co-occurrence network was built based on relationships of bacteria and fungi (top 30) (Fig. 2). Under their connectivity degree size ranking, eight nodes, namely *Alternaria*, *Botrytis*, *Kazachstania*, *Acremonium*, *Mycosphaerella*, *Pediococcus*, *Gardnerella*, and *Schizothecium*, were identified as the core microbiota during mulberry wine fermentation (Fig. 2). Of the fungal taxa, *Alternaria* (connect = 10) boasted the highest degree of connectivity and played an active role in the fermentation of alcoholic beverages such as wine and beer by transmuting sugars into alcohol and other compounds (Wen et al., 2021). *Botrytis* (connect = 9), a fungus that infects grape berries, generated metabolites from its spores that instigated glycerol accumulation and sugar consumption, thereby regulating the oxidative balance pathway. Furthermore, these metabolites positively influenced yeast metabolism in wine and ameliorated wine flavor (Schueuermann et al., 2019). *Kazachstania* (connect = 8) was frequently detected in various

alcoholic beverages and deemed a critical genus in producing phenols and esters, which made a significant contribution to the evolution of aroma and taste during alcohol fermentation in mulberry wine (Lin et al., 2022). *Pediococcus* (connect = 8)—one of the customary lactic acid bacteria present in fermented foods—assists specific transporters for efficient sugar uptake and undergoes intricate metabolic processes involving the carbohydrate and amino acid metabolism in the realm of mulberry fermentation (Xiao et al., 2022). In the context of both homolactic and hetero-lactic fermentations, *Pediococcus* efficiently converts sugars into many secondary metabolites. These metabolites encompass lactic acid, ethanol, acetic acid, and carbon dioxide (Xiao et al., 2022). Studies have indicated that certain strains of *Kazachstania* can assimilate lactate and hydrolyze glucuronide, thereby providing metabolic substrates to hetero-lactic fermentation organisms, enabling them to generate substantial amounts of acetic acid from fructose (Moroni et al., 2011). Therefore, the core microbiota was intricately associated with producing distinctive aromas.

3.4. The correlation between microorganisms and physicochemical parameters

The core microbiota's production, accumulation, and succession are crucial in the variation of oenological parameters (Peng et al., 2021), including pH, total sugar, total acids, total soluble solids, and alcohol content. RDA was used to assess the correlation between oenological parameters and the core microbiota at different fermentation times (Fig. 3). The first typical axis explained 50.07 % of the variation in the core microbiota. The succession of core microbiota was a significant driver of changes in oenological parameters (Fig. 3). The correlation between *Acremonium*, *Kazachstania*, and *Pediococcus*, and alcohol during fermentation was notably positive, whereas their correlation with pH, total sugar, and total acid was relatively low. These findings suggest that *Kazachstania* and *Pediococcus* could facilitate alcohol production during fermentation (Lin et al., 2022; Xiao et al., 2022). Moreover, they may exhibit reduced sugar utilization and decreased susceptibility to pH fluctuations. *Alternaria* and *Botrytis* revealed a strong positive correlation with pH and TS, indicating that although they may have high utilization of sugars, they are susceptible to acid environment disturbance that induces a stress response in the population, leading to fluctuations in their abundance level (Schueuermann et al., 2019; Wen et al., 2021). Therefore, the core microbiota succession during fermentation enhances their adaptability to environmental changes and responds positively to environmental variations. Simultaneously, they maintain their functionality for the specific aromas produced, increasing the overall aromatic richness during mulberry wine fermentation (Peng et al., 2021).

3.5. Dynamic changes in volatile compounds during mulberry wine fermentation

A total of 125 volatile compounds were identified using HS-SPME-GC-MS during the semi-artificial inoculated fermentation of mulberry wine. Esters, alcohols, aldehydes, ketones, acids, alkanes, and others were the main categories (Table S1). Esters (51 kinds) accounted for the highest proportion, followed by 18 aldehydes. Notably, acetone—a key substance in mulberry wine fermentation—was facilitated by yeast cells utilizing alcohol dehydrogenase and acetaldehyde dehydrogenase enzymes in the glycolytic pathway. Acetone is further converted into acetaldehyde, which undergoes additional oxidation into acetic acid by acetaldehyde dehydrogenase. Furthermore, the citric acid cycle and amino acid metabolism also promote the generation of volatile acids, such as isovaleric acid and isobutyric acid, during mulberry wine fermentation (Permyakova et al., 2023; Xu et al., 2019). Thus, a relatively higher overall content of volatile acids in the later stages of fermentation may compromise the aroma harmony of mulberry wine. Next, PCA pattern discriminant analysis based on volatile compounds could clearly distinguish the samples fermented at different time points.

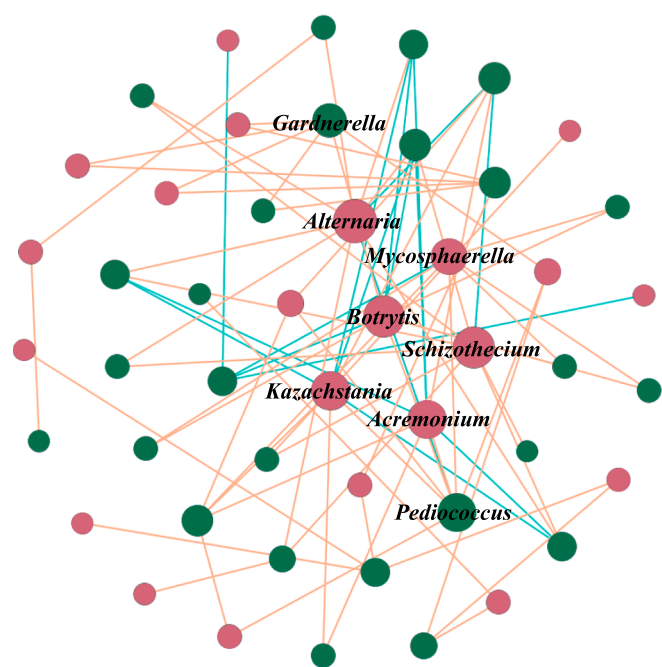


Fig. 2. The inter-kingdom network of bacterial and fungi. Red nodes represent fungi. Green nodes were bacterial. Red lines represent positive correlation. Blue lines represent negative correlation. The size of different nodes represents the connectivity strength, the larger the node the higher the connectivity, the smaller the node the lower the connectivity. Microbial taxa (*Alternaria*, *Botrytis*, *Kazachstania*, *Acremonium*, *Mycosphaerella*, *Pediococcus*, *Gardnerella*, and *Schizothecium*) with higher nodes were marked. (For interpretation of the references to colour in this figure legend, the reader is referred to the web version of this article.) (For interpretation of the references to colour in this figure legend, the reader is referred to the web version of this article.)

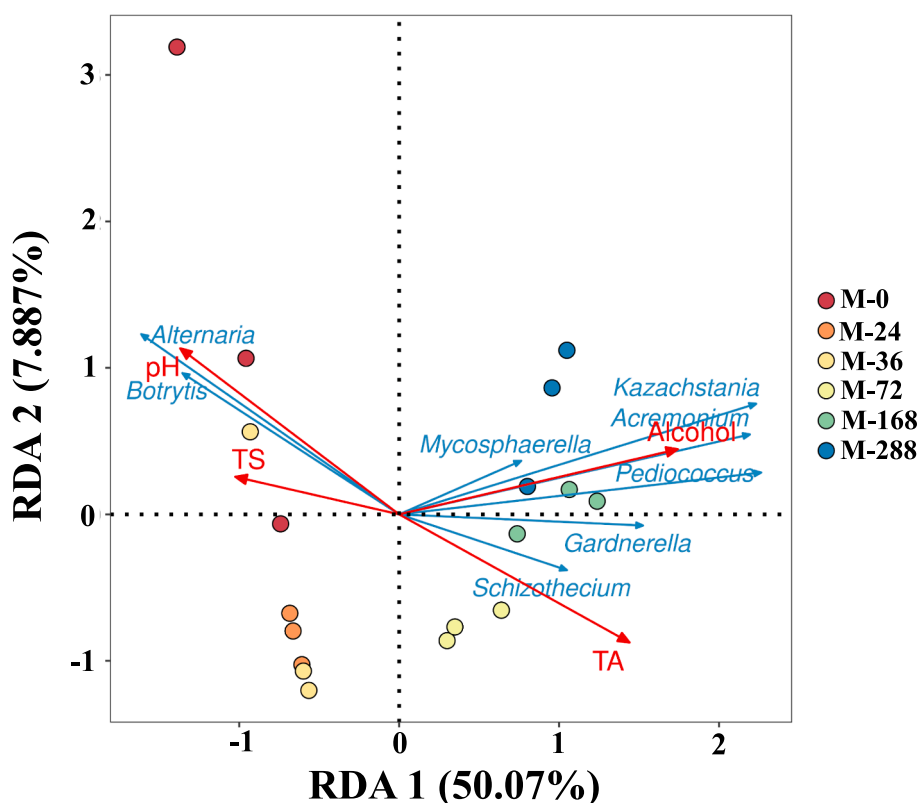


Fig. 3. Correlation between microbial community and physicochemical properties. RDA shows the correlation between physicochemical properties with the core microbiota communities. Red arrows represent different oenological parameter variables (pH; TS: Total Sugar; TA: Total Acids; Alcohol), blue arrows represent the core microbiota (*Alternaria*, *Botrytis*, *Kazachstania*, *Acremonium*, *Mycosphaerella*, *Pediococcus*, *Gardnerella*, and *Schizothecium*). Different colored circles represent samples of different time periods. (For interpretation of the references to colour in this figure legend, the reader is referred to the web version of this article.). (For interpretation of the references to colour in this figure legend, the reader is referred to the web version of this article.)

The two principal components expressed about 50.00 % of the total variance, with PC1 and PC2 accounting for 40.80 % and 9.20 %, respectively ($R^2X = 0.579$) (Fig. 4A). The results showed significant differences in volatile compound composition. Additionally, OPLS-DA analyses were implemented to explore the discriminatory volatile compounds contributing to distinguishing the different groups during fermentation ($R^2X = 0.818$, $R^2Y = 1$, $Q^2 = 0.995$) (Fig. 4B). A total of 79 distinguishing volatile compounds ($VIP > 1$, $Foldchange > 1.5$ or < 0.5 , $P < 0.05$) were detected among the 0-h and 288-h samples (Table S2). The detected volatile compounds consisted of six (five main) categories in terms of composition: esters (36 kinds), aldehydes (11 kinds), ketones (9 kinds), alcohols (8 kinds), alkanes (8 kinds), and others (7 kinds) (Fig. 4D).

The relative content of esters—the most prominent differential aroma compound—increased rapidly (Fig. 4C), 19.6-fold at 288 h (66.07 %) than at 0 h (3.37 %). The increase was mainly related to the acyltransferase enzyme, which was more active at low temperatures and conducive to ester accumulation (Chen et al., 2007). However, butanoic acid-methyl ester, 2-methyl-butanoic acid ethyl ester, butyrolactone, tetrahydro-6-methyl-2H-pyran-2-one, and ethyl oleate degrade gradually with fermentation, possibly resulting from chemical hydrolysis or volatilization loss (Sumbly et al., 2013). Notably, with a prolonged fermentation time, mulberry wine exhibited an increase in esters of $Foldchange > 2000$ ($VIP > 1$), such as ethyl format, acetic acid methyl ester, 3-methyl butyl butanoic acid ester, 2-hydroxy-2-methyl propyl-propanoic acid ester, ethane dioic acid, diethyl ester, diethyl malonate, diethyl adipate, and 9-oxo-nonanoic acid ethyl ester, with 2-hydroxy-propanoic acid ethyl ester being the most abundant volatile compound in the category.

Ketones and aldehydes—carbonyl-containing compounds formed by

alcohol oxidation and thermal degradation of carbohydrates—increased by 1.80 % and decreased by 2.96 %, respectively (Fig. 4C). Notably, at the end of fermentation (288 h), the differential volatile compounds 2-octanone, 1-hepten-3-one and 2, 3-hexanedione were tens of thousands-fold dramatic higher than those at 0 h (Supplementary Table S2). However, their overall percentage was not significant, probably because microorganisms possess aldo-keto reductases that promote the transfer of carbonyl groups to hydroxyl groups to form alcohols (Penning, 2015).

Alcohols—the precursors of aged esters—were derived mainly from sugars converted in fruit juices through central carbon metabolism and dehydrodecarboxylation of amino acids in yeasts and bacteria during alcoholic fermentation. The key enzymes involved in alcohol production were alcohol dehydrogenases (ADHs), which catalyze the conversion of sugars to alcohol (Qian et al., 2019). However, because of the esterification of alcohols, their relative content decreased from 84.10 % to 27.50 % (Fig. 4C; Supplementary Table S2). Furthermore, ethanol and 3-methyl-1-butanol were the primary alcohols in mulberry wine fermentation (Supplementary Table S2).

Alkanes are hydrocarbons synthesized from fatty acids via decarboxylation (Monteiro et al., 2022). Their relative content increased from 0.20 % to 1.20 %. Among them, 1,1-diethoxy-ethane, decane, and 1,1-diethoxy-pentane, as differential volatile compounds, were screened to the greatest relative content variation during mulberry wine fermentation (Fig. 4C; Supplementary Table S2).

The rOAV analysis was often used to assess the contribution of compounds to aroma performance. We used rOAV to determine the significance of volatile compounds in the fermentation process. Typically, a higher rOAV value indicates a greater contribution of a particular component to the overall flavor profile of the sample (Zhang et al.,

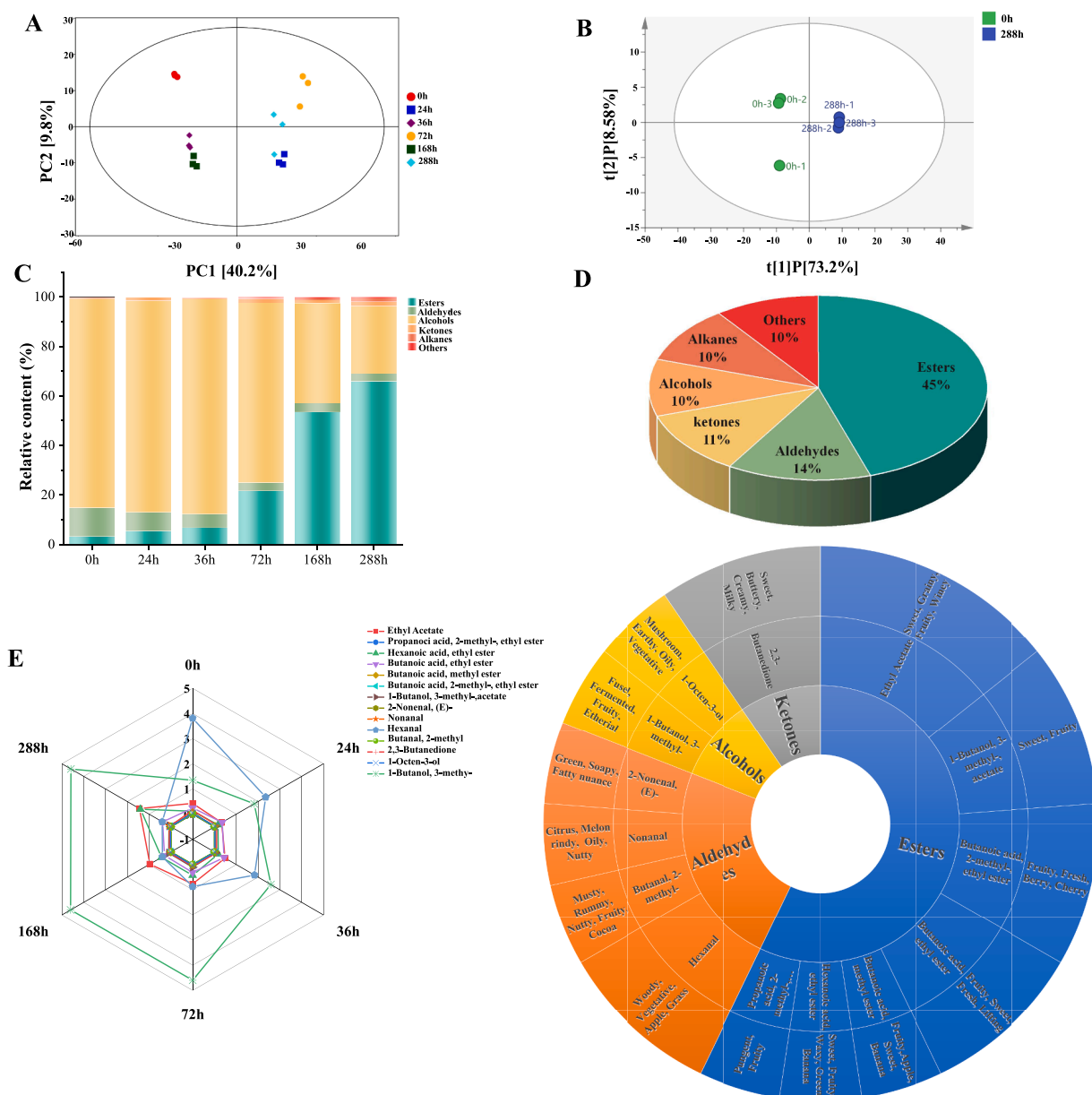


Fig. 4. The evolution analysis of volatile compounds during fermentation of mulberry wine. (A) Score scatter plot for PCA model (all); (B) Score scatter plot for OPLS-DA model (0 h vs 288 h); (C) The histogram of volatile compounds' content distribution (esters, aldehydes, ketones, alcohols, acids) with fermentation time (Top5 relative abundance (%) were identified); (D) Abundance stacking map of volatile compounds' change; (E) The variation of top five volatile compounds (esters, aldehydes, ketones, alcohols, alkanes) in terms of species and the secondary metabolites (14 kinds) in different time (0 h, 24 h, 36 h, 72 h, 168 h, 288 h). Classification of they belong, and the names of the fragrances contributed by the secondary metabolites. The description of all aroma characteristics was recorded in <http://www.thegoodscentscompany.com> and <https://mffi.sjtu.edu.cn/database>, 22th, Dec 2022.

2019).

In our study, 69 aroma compounds were selected based on recorded odor characteristics and rOAV (Supplementary Table S2). Among these, 14 compounds (rOAV > 1, VIP > 1, Foldchange > 1.5 or < 0.5, $P < 0.05$) were defined as key differential aromas compounds (Fig. 4E; Table S2). Among them, the following were the main contributing compounds to highlight the aroma of mulberry in terms of "Fruity", "Grass", and "Floral" (0 h): ethyl acetate (rOAV = 100), butanal, 2-methyl- (rOAV = 7.38), propanoic acid, 2-methyl-ethyl ester (rOAV = 9.99), butanoic acid methyl ester (rOAV = 1.11), butanoic acid ethyl ester (rOAV = 95.92), butanoic acid, 2-methyl-ethyl ester (rOAV = 95.92), 3-methyl-1-butanol acetate (rOAV = 50.68), hexanal (rOAV = 60.42), 2,3-butanedione (rOAV = 62.45), hexanoic acid, ethyl ester

(rOAV = 27.44), nonanal (rOAV = 3.55), 1-octen-3-ol (rOAV = 31.61), 2-nonenal, (E)- (rOAV = 4.14) and 1-butanol 3-methyl- (rOAV = 1.59) (Fig. 4E; Supplementary Table S2). With prolonged fermentation time, the aroma characteristics were substantially changed with environmental and microbial factors. For instance, the aromas of "Fruity", "Sweet", and "Grassy" became increasingly intense after 36 h of fermentation, blending with "Fresh" and "Lifting" notes. The aromatic characteristics of "Woody", "Buttery", "Milky", "Mushroom", "Earthy", and "Oily" gradually diminished throughout the fermentation process. Additionally, the aromas of "Fusel" and "Fermented" exhibited the most prominent growth in odor during the entire fermentation process. Remarkably, 1-hepten-3-one mainly contributed to "Mushroom" and was upregulated by 1428.57-fold (rOAV = 100) during the late

fermentation stage of the 288-h sample (Fig. 4E; Supplementary Table S2). Furthermore, the differential volatile compounds with $0 \leq \text{rOAV} \leq 1$ were considered to have a vital role in assisting the aroma development (acetaldehyde, ethane, 1,1-diethoxy-, 1-penten-3-one, 2,3-pentanedione, 1-penten-3-ol, 2-nonanone). Notably, “Nutty” and “Earthy” were assisted conferred in mulberry wine by 1, 1-dioxy ethane, an essential aroma coordination substance with aroma characteristics that were screened from the alkanes of fermented (288 h) berry wines for the first time ($\text{rOAV} = 0.58$). Semi-artificial inoculated fermentation significantly enriches and enhances the organoleptic attributes of wine (e.g., brandy and fruity flavors). Unlike it, spontaneous fermentation tends to increase the proportion of mid-aroma categories among total

volatile compounds, including alcohols and esters (Lu et al., 2020).

3.6. Correlation between the core microbiota and key differential aromas

The network of connecting (Pearson’s correlation coefficient, $r \geq 0.5$, $P < 0.05$) was constructed to determine the correlation between the core microbiota and key differential aromas (Fig. 5), which mainly contributed to predicting the roles of microbiota in differential aroma formation during mulberry wine fermentation. *Botrytis*, *Acremonium*, *Kazachstania*, *Pediococcus*, and *Alternaria* demonstrated a robust correlation with the key differential aromas (Fig. 5). Among them, the relative abundance of *Pediococcus* was low (0.03 %-0.04 %) and remained

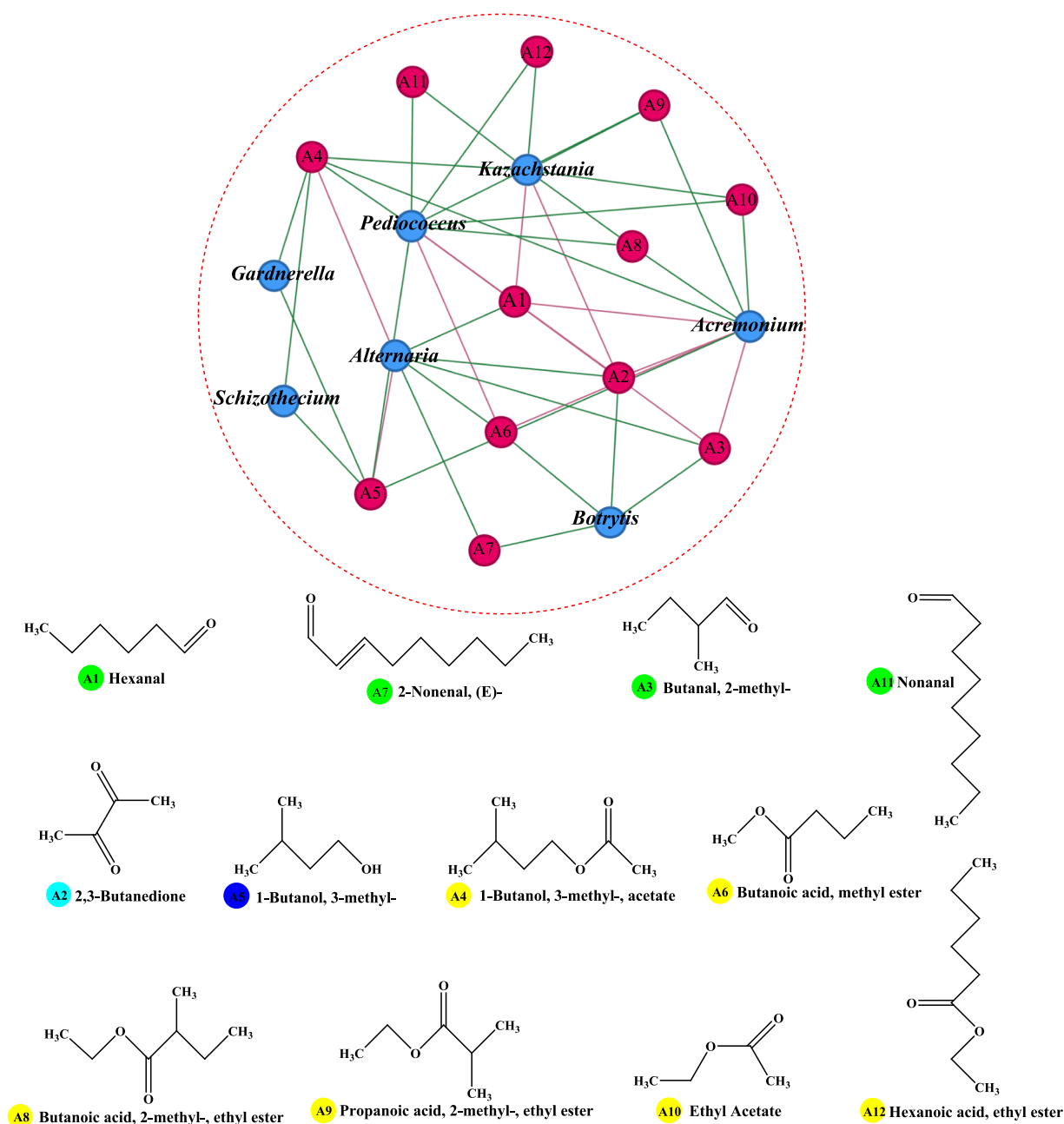


Fig. 5. The relationship network between (19 nodes; 44 edges; Pearson: $r \geq 0.5$, $p < 0.05$) the core microbiota and key different aroma. Red nodes represent key volatile aroma compounds, blue nodes represent the core microbiota. Pink lines represent negative correlation, green lines represent positive correlation. The size of the nodes indicates the magnitude of their connectivity (degree). The Structure Diagram of 12 key aromas compounds, which related with the core tax of micro-organism out of red circle. The different colors of nodes represent the different compounds corresponding to the diagram (Yellow: esters; Green: aldehydes; Low blue: ketones; Deep blue: alcohols). (For interpretation of the references to colour in this figure legend, the reader is referred to the web version of this article.)

stable during the 72-h period. The following key differential aromas were detected in the early stages and were positively associated with *Pediococcus*: 1-butanol, 3-methyl-acetate (A4, “Fruity” and “Sweet”), 1-butanol, 3-methyl- (A5, “Fusel” and “fermented”), propanoic acid, 2-methyl-ethyl ester (A9, “Pungent and Fruity”), ethyl acetate (A10, “Fruity” and “Sweet”), nonanal (A11, “Fruity” and “Oily”), and hexanoic acid ethyl ester (A12, “Sweet” and “Fruity”). By contrast, hexanal (A1, “Woody”), 2,3-butanedione (A2, “Buttery” and “Milky”), butanal, 2-methyl- (A3, “Musty”, “Rummy”, and “Nutty”), and butanoic acid, methyl ester (A6, “Fruity” and “Sweet”), exhibited decreasing trend and were negatively correlated. Additionally, *Kazachstania* possessed the same positively correlated key differential aroma as *Pediococcus*. From 72 to 288 h of fermentation, the relative abundance of *Pediococcus* increased from 1.20 % to 1.70 %, respectively. Concurrently, the compounds responsible for the distinctive differential aromas in mulberry wine started emitting more pronounced fragrances. Furthermore, fluctuations in the relative abundance of *Kazachstania* and its positive correlation with key differential aromas mirrored those observed in *Pediococcus*. However, *Kazachstania* exhibited a negative correlation exclusively with aldehydes and ketones among the key differential aromas. Specifically, as the percentage of *Kazachstania* increased, there was a gradual decline in the woody, buttery, and milky aroma attributed to hexanal (A1) and 2,3-butanedione (A2) in mulberry wine. Moreover, the synergistic interaction between *Kazachstania* and *Pediococcus* may facilitate the development of specific key differential aromas (Xiao et al., 2022), including “Fruity”, “Sweet”, “Grassy”, and “Lifting”. Previous studies also revealed that *Kazachstania* was a core microbiota associated with flavor (e.g., alcohols and esters) formation during flat peach wine fermentation (Xu et al., 2022), *Pediococcus* was highly responsible for producing flavor substances (ethyl laurate, acetic acid) in Shaoxing-jiu (Chen et al., 2020). Notably, *Alternaria* and *Botrytis*, as common spoilage bacteria, exhibited a similar positive correlation with aroma-forming substances such as butanoic acid, methyl ester (A6), 2-nonenal, (E)-(A7), hexanal (A1), butanal, 2-methyl-(A3) in our study. The certain contribution of natural spoilage bacteria to fruit wine aroma (“Stone” and “Cheese”) during semi-artificial inoculation fermentation may be explained by this correlation (Schueuermann et al., 2019; Wen et al., 2021).

4. Conclusion

In our study, lactic acid bacteria (*Lactobacillus* and *Pediococcus*) were identified as the predominant bacterial groups during mulberry wine fermentation. In the fungal kingdom, fermentation yeasts (*Kazachstania*, *Issatchenkia*, *Saccharomyces*, and *Wickerhamomyces*) were crucial in shaping the course of fermentation. Moreover, the core microbiota of eight closely interconnected taxonomic units were identified using inter-kingdom correlation networks. In light of aroma analysis, 14 aroma compounds were identified as key differentiating ones. The correlation analysis between key differentiating aroma and microorganisms demonstrated that the microorganisms were the imperative contributors to aroma production during mulberry wine fermentation. Our findings can enhance our understanding of the production mechanisms of flavored beverages, particularly fruit wines.

CRedit authorship contribution statement

Yanan Qin: Writing – review & editing, Supervision, Resources, Project administration, Funding acquisition. **Haotian Xu:** Writing – review & editing, Writing – original draft, Methodology, Investigation, Formal analysis, Data curation, Conceptualization. **Jinshuai Sun:** Writing – review & editing, Data curation. **XiangYang Cheng:** Data curation. **Jing Lei:** Funding acquisition. **Weijia Lian:** Funding acquisition. **Chen Han:** Investigation. **Wanting Huang:** Data curation. **Minwei Zhang:** Writing – original draft. **Ya Chen:** Writing – review & editing, Funding acquisition, Conceptualization.

Declaration of competing interest

The authors declare that they have no known competing financial interests or personal relationships that could have appeared to influence the work reported in this paper.

Data availability

Data will be made available on request.

Acknowledgments

This work was supported by the Natural Science Foundation of Xinjiang (No.2022D01B34, No.2022D01C404, No.2022D01D42), Tianshan Youth Project in Xinjiang Autonomous Region (No. 2019Q002), University Scientific Research Project in Education Department of Xinjiang Autonomous Region (No. XJEDU2020Y009), the research start-up fund of Xinjiang University (No. 2018-660010) and QY acknowledges Tianchi doctoral program (No.2020660024).

Appendix A. Supplementary data

Supplementary data to this article can be found online at <https://doi.org/10.1016/j.fochx.2024.101223>.

References

- Cason, E. D., Mahlomaholo, B. J., Taole, M. M., Abong, G. O., Vermeulen, J. G., De Smidt, O., Vermeulen, M., Steyn, L., Valverde, A., & Viljoen, B. (2020). Bacterial and fungal dynamics during the fermentation process of Sesotho, a traditional beer of southern Africa. *Frontiers in Microbiology*, 11, 1451. <https://doi.org/10.3389/fmicb.2020.01451>
- Carpena, M., Fraga-Corral, M., Otero, P., Nogueira, R. A., Garcia-Oliveira, P., Prieto, M. A., & Simal-Gandara, J. (2021). Secondary aroma: Influence of wine microorganisms in their aroma profile. *Foods*, 10, 51. <https://doi.org/10.3390/foods10010051>
- Chen, C., Liu, Y., Tian, H., Ai, L., & Yu, H. (2020). Metagenomic analysis reveals the impact of JIUYAO microbial diversity on fermentation and the volatile profile of Shaoxing-jiu. *Food Microbiology*, 86, Article 103326. <https://doi.org/10.1016/j.fm.2019.103326>
- Chen, Q., Steinhauer, L., Hammerlindl, J., Keller, W., & Zou, J. (2007). Biosynthesis of phytosterol esters: Identification of a sterol O -Acyltransferase in Arabidopsis. *Plant Physiology*, 145(3), 974–984. <https://doi.org/10.1104/pp.107.106278>
- Ekumah, J. N., Ma, Y., Akpabli-Tsigbe, N. D. K., Kwaw, E., Jie, H., Quaisie, J., Manqing, X., & Johnson Nkuma, N. A. (2021). Effect of selenium supplementation on yeast growth, fermentation efficiency, phytochemical and antioxidant activities of mulberry wine. *LWT-Food Science and Technology*, 146, Article 111425. <https://doi.org/10.1016/j.lwt.2021.111425>
- Ercisli, S., & Orhan, E. (2007). Chemical composition of white (*Morus alba*), red (*Morus rubra*) and black (*Morus nigra*) mulberry fruits. *Food Chemistry*, 103(4), 1380–1384. <https://doi.org/10.1016/j.foodchem.2006.10.054>
- Escribano-Viana, R., González-Arenzana, L., Portu, J., Garijo, P., López-Alfaro, I., López, R., Santamaría, P., & Gutiérrez, A. R. (2018). Wine aroma evolution throughout alcoholic fermentation sequentially inoculated with non-*Saccharomyces*/*Saccharomyces* yeasts. *Food Research International*, 112, 17–24. <https://doi.org/10.1016/j.foodres.2018.06.018>
- García, A., & Barbas, C. (2011). Gas chromatography-mass spectrometry (GC-MS)-based metabolomics. *Methods in Molecular Biology*, 2011(708), 191–204. https://doi.org/10.1007/978-1-61737-985-7_11
- Hosseini, A. S., Akramian, M., Khadivi, A., & Salehi-Arjmand, H. (2018). Phenotypic and chemical variation of black mulberry (*Morus nigra*) genotypes. *Industrial Crops and Products*, 117, 260–271. <https://doi.org/10.1016/j.indcrop.2018.03.007>
- Hu, J., Vinothkanna, A., Wu, M., Ekumah, J., Akpabli-Tsigbe, N. D. K., & Ma, Y. (2021). Tracking the dynamic changes of a flavor, phenolic profile, and antioxidant properties of *Lactiplantibacillus plantarum* - and *Saccharomyces cerevisiae* -fermented mulberry wine. *Food Science & Nutrition*, 9(11), 6294–6306. <https://doi.org/10.1002/fsn3.2590>
- Jiang, Y., & Nie, W. J. (2015). Chemical properties in fruits of mulberry species from the Xinjiang province of China. *Food Chemistry*, 174, 460–466. <https://doi.org/10.1016/j.foodchem.2014.11.083>
- Liang, L., Ma, Y., Jiang, Z., Sam, F. E., Peng, S., Li, M., & Wang, J. (2023). Dynamic analysis of microbial communities and flavor properties in Merlot wines produced from inoculation and spontaneous fermentation. *Food Research International*, 164, Article 112379. <https://doi.org/10.1016/j.foodres.2022.112379>
- Lin, M. M. H., Boss, P. K., Walker, M. E., Sumbly, K. M., & Jiranek, V. (2022). Influence of *Kazachstania* spp. On the chemical and sensory profile of red wines. *International Journal of Food Microbiology*, 362, Article 109496. <https://doi.org/10.1016/j.ijfoodmicro.2021.109496>

- Liu, C., Li, M., Ren, T., Wang, J., Niu, C., Zheng, F., & Li, Q. (2022). Effect of *Saccharomyces cerevisiae* and non-*Saccharomyces* strains on alcoholic fermentation behavior and aroma profile of yellow-fleshed peach wine. *LWT-Food Science and Technology*, 155, Article 112993. <https://doi.org/10.1016/j.lwt.2021.112993>
- Liu, W. H., Chai, L. J., Wang, H. M., Lu, Z. M., Zhang, X. J., Xiao, C., Wang, S. T., Shen, C. H., Shi, J. S., & Xu, Z. H. (2023). Bacteria and filamentous fungi running a relay race in Daqu fermentation enable macromolecular degradation and flavor substance formation. *International Journal of Food Microbiology*, 390, Article 110118. <https://doi.org/10.1016/j.ijfoodmicro.2023.110118>
- Lu, Y., Liu, Y., Lv, J., Ma, Y., & Guan, X. (2020). Changes in the physicochemical components, polyphenol profile, and flavor of persimmon wine during spontaneous and inoculated fermentation. *Food Science & Nutrition*, 8, 2728–2738. <https://doi.org/10.1002/fsn3.1560>
- Monteiro, R. R. C., Da Silva, S. S. O., Cavalcante, C. L., De Luna, F. M. T., Bolivar, J. M., Vieira, R. S., & Fernandez-Lafuente, R. (2022). Biosynthesis of alkanes/alkenes from fatty acids or derivatives (triacylglycerols or fatty aldehydes). *Biotechnology Advances*, 61, Article 108045. <https://doi.org/10.1016/j.biotechadv.2022.108045>
- Moroni, A. V., Arendt, E. K., & Bello, F. D. (2011). Biodiversity of lactic acid bacteria and yeasts in spontaneously-fermented buckwheat and teff sourdoughs. *Food Microbiology*, 28(3), 497–502. <https://doi.org/10.1016/j.fm.2010.10.016>
- Peng, M. Y., Zhang, X. J., Huang, T., Zhong, X. Z., Chai, L. J., Lu, Z. M., Shi, J. S., & Xu, Z. H. (2021). *Komagataeibacter europaeus* improves community stability and function in solid-state cereal vinegar fermentation ecosystem: Non-abundant species plays important role. *Food Research International*, 150, Article 110815. <https://doi.org/10.1016/j.foodres.2021.110815>
- Penning, T. M. (2015). The aldo-keto reductases (AKRs): Overview. *Chemico-Biological Interactions*, 234, 236–246. <https://doi.org/10.1016/j.cbi.2014.09.024>
- Permyakova, L., Sergeeva, I., Dolgolyuk, I., Starovoitova, K., Atuchin, V., Vereshchagin, A., Romanenko, V., & Lashitsky, S. (2023). Combined effect of ultrasound treatment and a mix of krebs cycle acids on the metabolic processes in *Saccharomyces cerevisiae*. *Fermentation*, 9, 132. <https://doi.org/10.3390/fermentation9020132>
- Qian, X., Liu, Y., Zhang, G., Yan, A., Wang, H., Wang, X., Pan, Q., Xu, H., Sun, L., & Zhu, B. (2019). Alcohol acyltransferase gene and ester precursors differentiate composition of volatile esters in three interspecific hybrids of *Vitis labrusca* × *V. Vinifera* during berry development period. *Food Chemistry*, 295, 234–246. <https://doi.org/10.1016/j.foodchem.2019.05.104>
- Qin, Y., Xu, H., Chen, Y., Lei, J., Sun, J., Zhao, Y., Lian, W., & Zhang, M. (2023). Metabolomics-based analyses of dynamic changes in flavonoid profiles in the black mulberry winemaking process. *Foods*, 12(11), 2221. <https://doi.org/10.3390/foods12112221>
- Ristic, R., Danner, L., Johnson, T. E., Meiselman, H. L., Hoek, A. C., Jiranek, V., & Bastian, S. E. P. (2019). Wine-related aromas for different seasons and occasions: Hedonic and emotional responses of wine consumers from Australia, UK and USA. *Food Quality and Preference*, 71, 250–260. <https://doi.org/10.1016/j.foodqual.2018.07.011>
- Schueuermann, C., Steel, C. C., Blackman, J. W., Clark, A. C., Schwarz, L. J., Moraga, J., Collado, I. G., & Schmidtke, L. M. (2019). A GC–MS untargeted metabolomics approach for the classification of chemical differences in grape juices based on fungal pathogen. *Food Chemistry*, 270, 375–384. <https://doi.org/10.1016/j.foodchem.2018.07.057>
- Su, C., Zhang, K. Z., Cao, X. Z., & Yang, J.-G. (2020). Effects of *Saccharomycopsis fibuligera* and *Saccharomyces cerevisiae* inoculation on small fermentation starters in Sichuan-style Xiaoyu liquor. *Food Research International*, 137, Article 109425. <https://doi.org/10.1016/j.foodres.2020.109425>
- Summy, K. M., Jiranek, V., & Grbin, P. R. (2013). Ester synthesis and hydrolysis in an aqueous environment, and strain specific changes during malolactic fermentation in wine with *Oenococcus oeni*. *Food Chemistry*, 141(3), 1673–1680. <https://doi.org/10.1016/j.foodchem.2013.03.087>
- Teng, T. S., Chin, Y. L., Chai, K. F., & Chen, W. N. (2021). Fermentation for future food systems: Precision fermentation can complement the scope and applications of traditional fermentation. *EMBO Reports*, 22(5), e52680.
- Tian, X., Chen, H., Liu, H., & Chen, J. (2021). Recent Advances in Lactic Acid Production by Lactic Acid Bacteria. *Applied Biochemistry and Biotechnology*, 193(12), 4151–4171. <https://doi.org/10.1007/s12010-021-03672-z>
- Wang, Y., Wu, J., Lv, M., Shao, Z., Hungwe, M., Wang, J., Bai, X., Xie, J., Wang, Y., & Geng, W. (2021). Metabolism characteristics of lactic acid bacteria and the expanding applications in food industry. *Frontiers in Bioengineering and Biotechnology*, 9, Article 612285. <https://doi.org/10.3389/fbioe.2021.612285>
- Wang, Z., Feng, Y., Yang, N., Jiang, T., Xu, H., & Lei, H. (2022). Fermentation of kiwifruit juice from two cultivars by probiotic bacteria: Bioactive phenolics, antioxidant activities and flavor volatiles. *Food Chemistry*, 373, Article 131455. <https://doi.org/10.1016/j.foodchem.2021.131455>
- Wei, R., Chen, N., Ding, Y., Wang, L., Liu, Y., Gao, F., Zhang, L., Li, H., & Wang, H. (2022). Correlations between microbiota with physicochemical properties and volatile compounds during the spontaneous fermentation of Cabernet Sauvignon (*Vitis vinifera* L.) wine. *LWT-Food Science and Technology*, 163, Article 113529. <https://doi.org/10.1016/j.lwt.2022.113529>
- Wen, R., Li, X., Han, G., Chen, Q., & Kong, B. (2021). Fungal community succession and volatile compound dynamics in Harbin dry sausage during fermentation. *Food Microbiology*, 99, Article 103764. <https://doi.org/10.1016/j.fm.2021.103764>
- Xiao, R., Chen, S., Wang, X., Chen, K., Hu, J., Wei, K., Ning, Y., Xiong, T., & Lu, F. (2022). Microbial community starters affect the profiles of volatile compounds in traditional Chinese Xiaoyu rice wine: Assessment via high-throughput sequencing and gas chromatography-ion mobility spectrometry. *LWT-Food Science and Technology*, 170, Article 114000. <https://doi.org/10.1016/j.lwt.2022.114000>
- Xu, X., Miao, Y., Wang, H., Ye, P., Li, T., Li, C., Zhao, R., Wang, B., & Shi, X. (2022). A snapshot of microbial succession and volatile compound dynamics in flat peach wine during spontaneous fermentation. *Frontiers in Microbiology*, 13, Article 919047. <https://doi.org/10.3389/fmicb.2022.919047>
- Xu, X., Niu, C., Liu, C., & Li, Q. (2019). Unraveling the mechanisms for low-level acetaldehyde production during alcoholic fermentation in *Saccharomyces pastorianus* lager yeast. *Journal of Agricultural and Food Chemistry*, 67(7), 2020–2027. <https://doi.org/10.1021/acs.jafc.8b06868>
- Yang, X., Zhao, F., Yang, L., Li, J., & Zhu, X. (2022). Enhancement of the aroma in low-alcohol apple-blended pear wine mixed fermented with *Saccharomyces cerevisiae* and non-*Saccharomyces* yeasts. *LWT-Food Science and Technology*, 155, Article 112994. <https://doi.org/10.1016/j.lwt.2021.112994>
- Yuan, W., Du, Y., Yu, K., Xu, S., Liu, M., Wang, S., Yang, Y., Zhang, Y., & Sun, J. (2022). The production of pyruvate in biological technology: A critical review. *Microorganisms*, 10(12), 2454. <https://doi.org/10.3390/microorganisms10122454>
- Zhang, W., Dong, P., Lao, F., Liu, J., Liao, X., & Wu, J. (2019). Characterization of the major aroma-active compounds in Keitt mango juice: Comparison among fresh, pasteurization and high hydrostatic pressure processing juices. *Food Chemistry*, 289, 215–222. <https://doi.org/10.1016/j.foodchem.2019.03.064>
- Zhang, S., Xing, X., Chu, Q., Sun, S., & Wang, P. (2022). Impact of co-culture of *Lactobacillus plantarum* and *Oenococcus oeni* at different ratios on malolactic fermentation, volatile and sensory characteristics of mulberry wine. *LWT-Food Science and Technology*, 69, Article 113995. <https://doi.org/10.1016/j.lwt.2022.113995>